The 9th European Congress on Computational Methods in Applied Sciences and Engineering
ECCOMAS Congress 2024
3–7 June 2024, Lisboa, Portugal

LIQUID HEAVY METAL APPLICATIONS FOR PARTICLE ACCELERATORS

GIACOMO BARBI[1], CARLO CARRELLI[2], ANTONIO CERVONE[1], TOMMASO DEL MORO[2], IVAN DI PIAZZA[2], FEDERICO GIANGOLINI[1], SANDRO MANSERVISI[1], PIETRO CIOLI PUVIANI[2], LUCIA SIROTTI[1] AND LUCA TRICARICO[1]

[1] Department of Industrial Engineerign (DIN)
Alma Mater Studiorum University of Bologna
Montecuccolino Laboratory, Via dei Colli 16, 40136 Bologna, Italy
www.ingegneriaindustriale.unibo.it

[2] Italian National Agency for New Technologies, Energy and Sustainable Economic Development (ENEA)
Brasimone ENEA Research Center
Località Brasimone, 40032 Camugnano, Bologna, Italy
www.brasimone.enea.it

Key words: CFD, Liquid Heavy Metal, Particle Accelerators, Beam Dump Facility

Summary. *Lead possesses high density and excellent heat capacity, making it an ideal candidate for managing high power densities across various fields. Revitalized applications of this heavy liquid metal as a coolant in Generation IV nuclear reactors have opened new possibilities, including its use as an operating fluid in particle accelerators, where it becomes a target for laser beams. This study is carried out considering liquid lead in an alternative design for the Super Proton Synchrotron (SPS) Beam Dump Facility (BDF) at the European Laboratory for Particle Physics (CERN). Computational Fluid Dynamics (CFD) analysis are conducted with various codes to depict the liquid lead behaviour and predict the temperature field on the target vessel induced by the beams, modelled as a heat source acting on the target volume. We consider a pulsed proton laser beam hitting the target every* 7.2 *seconds with an average deposited power of* 355 *kW and a* 400 *GeV/c momentum. The charged beam data are provided by CERN through a Monte Carlo analysis of beam-lead interaction simulations.*

1 INTRODUCTION

Recent advancements in spallation sources for high-power beam facilities have led to the developing of systems capable of handling substantial energy deposition in short bursts. These systems necessitate innovative design strategies to mitigate the detrimental effects of intense heat and radiation on target materials. Traditional solid-state targets, like those used in the Super Proton Synchrotron Beam Dump Facility (SPS-BDF) at CERN, are increasingly challenged by the escalating energy demands, requiring efficient cooling mechanisms and managing of high thermal and mechanical stresses. In response, there is a growing interest in exploring alternative target designs that can better accommodate these extreme conditions.

This paper proposes a novel approach for the SPS-BDF, utilizing a flowing liquid lead target, operating at approximately 400° C, as a replacement for the conventional solid-state one. To reduce overheating, thus unwanted effects and failures while ensuring efficient cooling and high beam density, the proposed design considers moving the target material out of the reaction zone to remove heat elsewhere. Liquid metals offer substantial thermal capacity and enhanced cooling efficiency, potentially providing a more robust solution for high-energy deposition environments. However, adopting liquid metal targets introduces unique challenges, especially in the accurate simulation of turbulent heat transfer due to the distinct physical properties of liquid metals, such as low Prandtl numbers.

To investigate the feasibility of this alternative design, we conduct a comprehensive study using Computational Fluid Dynamics (CFD) simulations, employing two leading commercial codes: ANSYS Fluent and ANSYS CFX. These simulations are configured with carefully matched initial, boundary conditions and turbulent models to facilitate a direct comparison between the two software packages. Our focus is on accurately capturing the complex thermal and fluid dynamics within the proposed liquid lead target when hit by the full beam power, which is crucial for assessing its performance and viability in the SPS-BDF setting. Three different classes of simulations have been conducted: (1) En_T, where only the energy equation with imposed motion is solved; (2) En_Tm, where only the energy equation with variable physical properties is solved; (3) En_full, where the complete simulation with variable properties, equation of motion, and energy are solved. Moreover, the analysis is performed for two consequent beams to investigate the temperature dependence on frequency. By providing a comparative analysis of Fluent and CFX results, this study aims to give insights into the potential of liquid metal targets in high-power proton beam facilities and to guide future developments in particle accelerators.

2 THE FACILITY AND THE TARGET

The SPS-BDF at the European Laboratory for Particle Physics (CERN) is a facility intended for both beam-dump-like and fixed target experiments, searching for very weak particles such as the “tau neutrino” in the realm of the SHiP Project [1]. Its current working principle is based on a high-energy pulsed proton beam hitting a solid-state target, made of high-Z material with a short nuclear interaction length. In Figure 1 we can see the full target facility assembly and an insight into the solid-state target, made of Titanium-zirconium-doped molybdenum alloy-tungsten (TZM-W) in cylindrical blocks’ configuration, cooled thanks to high-velocity pressurized and demineralized flowing water. Assembly challenges were encountered, and operational as well. Despite the building issues with solid-state blocks, the primary concern was the target’s handling of full beam power. The solid-state target is required to safely withstand and absorb an average proton beam of 355 kW, with a 1/7.2 Hz frequency and a 400 GeV/c momentum, avoiding premature failure by cracking due to the high energy density deposition. In 2018 primary tests on the target were conducted [3], resulting in a successful handling of the beam power only when diluted, meaning moving the beam spot location magnetically over the pulse time.

These challenges led us to consider a new baseline target made of flowing liquid metals, to increase the maximum tolerable power and its handling capability while reducing the target degradation and loss of functionality due to thermo-mechanical stresses. In particular, this paper investigates the use of flowing liquid lead as a new concept target for the SPS-BDF.

Applications of heavy liquid metals as coolant in Generation IV nuclear reactors opened new possibilities exploiting their large thermal capacity and high boiling point, therefore guaranteeing a larger safety margin in operations. The proposed target geometry is shown in Figure 2. It is made of a cylindrical volume of 150 millimetres diameter and 2 meters long with liquid lead flowing inside it. The metal enters (with a 400 ° C temperature) and exits the tube through two cylindrical nozzles, with a 76 mm diameter. The pipe dimensions recall the computational domain in which the Monte Carlo simulations conducted by CERN for the beam thermal source took place. As the image highlights, the beam is hitting the target on its right-most side.

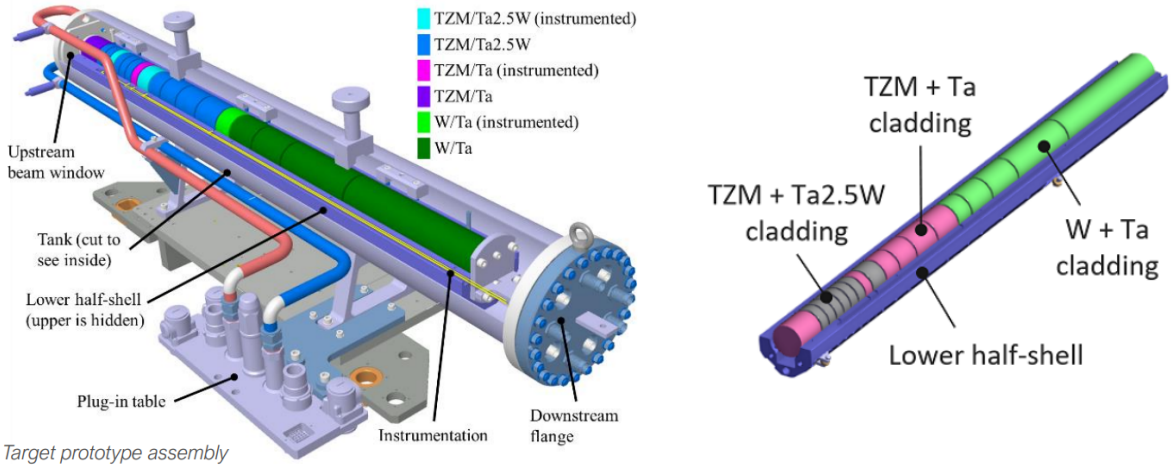

Figure 1: SPS-BDF assembly and a particular on its solid-state target on the right. Figures taken from [2] (left), [3] (right).

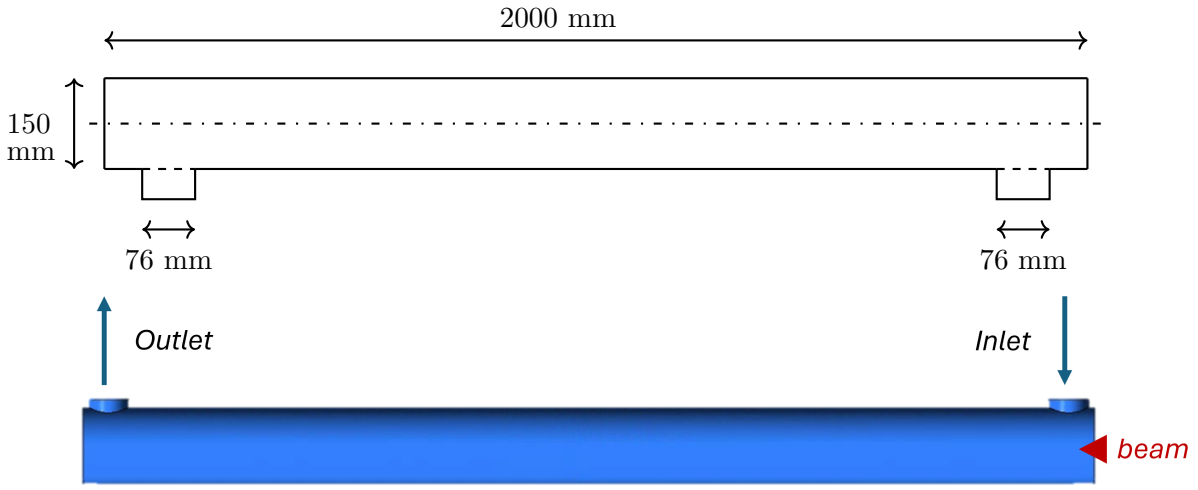

Figure 2: Quotes and representation of the proposed new domain.

3 LIQUID METALS MODELLING

In recent years, Heavy Liquid Metals found renewed interest in the scientific community. Due to their high density, high thermal conductance and heat capacity, they result in an extremely efficient mechanism of heat disposal, making them attractive for applications where significant temperature and heat flux take place and need to be removed. Such examples can be their use as cooling fluids in Generation IV nuclear power plants, solar collectors, and materials for the spallation target in accelerator-driven systems (ADS). The current section then provides an analysis of the lead properties correlations together with the mathematical model for turbulent heat transfer and the corresponding numerical implementation. The employed thermophysical properties of Lead are defined by the correlation taken from [4]. These are temperature-dependent, and valid in the range between lead melting and boiling point (respectively, 600 K and 2021 K):

$$\begin{aligned} \rho\,[kg\,m^{-3}] &= 11441 - 1.2795\,T\,, \\ \mu\,[Pa\,s] &= 4.55\cdot 10^{-4}\,exp(1069/T)\,, \\ k\,[W\,m^{-1}\,K^{-1}] &= 9.2 + 0.011T\,, \\ C_p\,[J\,K^{-1}kg^{-1}] &= 176.2 - 4.923\cdot 10^{-2}\,T + 1.544\cdot 10^{-5}\,T^2 - 1.524\cdot 10^{6}\,T^{-2}\,. \end{aligned} \tag{1}$$

where ρ is the density, μ the molecular viscosity, k the thermal conductivity and C_p the specific heat. The challenges associated with accurate temperature modeling through CFD come up when dealing with liquid metals. The causes can be found in their very different thermal and momentum diffusivity, with the former contribution largely overcoming the latter, resulting in low Prandtl numbers, on the scale $0.001 - 0.03$. This is in contrast to "conventional fluids", such as air and water, where the two diffusivity terms are comparable, thus $Pr \sim 0.8$ - 1. Mostly, commercial codes such as Fluent and CFX fail to evaluate heat transfer dynamics in turbulent regimes with liquid metals since they are equipped with turbulence models validated for almost unitary Pr number only. This paradigm is based on considering a constant value of turbulent Prandtl number, $Pr_t = \nu_t/\alpha_t$, thus closing the turbulent energy equations calculating the turbulent thermal diffusivity as $\alpha_t = Pr\,\nu_t$. However, this assumption does not hold for liquid metals, hence a more advanced model is necessary to accurately simulate heat transfer in these fluids. In many cases, the implementation of new turbulence models within the source code of commercial software is not possible, thus different approaches need to be taken into account. A possibility is to rely on CFD simulations carried on with DNS (Direct Numerical Simulations) that calculate numerically the exact values of the heat transfer coefficient. This would allow the best modelling of thermal phenomena without the need for experimental facility, but the calculations are limited to small geometries due to the extremely high computational cost involved. Another approach is to model the turbulent Prandtl number as a function of geometry and some dimensionless quantity defining the motion. This approach would still result in a constant Pr_t (when fixed the geometry and the regime) but it offers more accurate results with minimal implementation effort, that lightly affects the PDE system of equations. However, one of the primary limitations is that these correlations are valid for a limited range of geometries. In this paper, this latter solution has been chosen since these correlations exist for simple geometrical configurations such as the cylindrical channel, adopted in our study. The turbulent Prandtl number is hence defined in the CFD codes exploiting the correlations from

[5]:

$$Pr_t\,(b, Pe) = \frac{0.01\,Pe}{(0.018\,Pe^{0.8} - 7\,b)^{1.25}} \qquad 1000 \leq Pe \leq 6000\,, \tag{2}$$

where Pe is the Péclet number, defined as the product $Pe = Re\,Pr$ with Re the Reynolds number and b given by

$$b = \begin{cases} 4.5 & Pe \leq 1000 \\ 5.4 - 9 \cdot 10^{-4}\,Pe & 1000 \leq Pe \leq 2000 \\ 3.6 & Pe \geq 2000\,. \end{cases} \tag{3}$$

4 SOURCE DEFINITION

The thermal source generated by the proton beam plays a crucial role in the system's overall heat transfer dynamics. When protons interact with the target material, they deposit energy along their path, creating localized regions of intense heat. This leads to a highly non-uniform thermal field, which poses significant challenges for accurate modelling and simulation. In our computational models, the heat source from the proton beam is represented as a volumetric heat generation term, which varies along the target length. This section examines the details of how the proton beam's thermal source is represented in our models and the challenges associated with its numerical implementation in the CFD codes. The proton beam distribution in Cartesian coordinates (x, y, z) is provided by CERN and has been evaluated using the Monte Carlo code FLUKA[6]. The distribution is axisymmetric along x and y directions, where it follows a Gaussian profile, while in the z direction it peaks with an exponential behaviour. The source minimum (Min), maximum (Max), and average (Ave) distribution are listed in Table 1, as well as the source intensity in W/m^3, while its characteristics are wrapped up in Table 2.

Table 1: Thermal source data from the proton beam, in Cartesian coordinates.

	x [m]	y [m]	z [m]	S [W m^{-3}]
Min	$-7.3 \cdot 10^{-2}$	$-7.3 \cdot 10^{-2}$	$2.5 \cdot 10^{-3}$	$1.2 \cdot 10^{5}$
Max	$7.3 \cdot 10^{-2}$	$7.3 \cdot 10^{-2}$	2	$5.9 \cdot 10^{9}$
Ave	–	–	–	$7.2 \cdot 10^{7}$

Table 2: Values for the characterizing properties of the proton beam.

Quantity	Value	Unit of Measure
Pulse power	$1.81 \cdot 10^{6}$	W
Pulse energy	$1.81 \cdot 10^{6}$	J
Average power	$2.52 \cdot 10^{5}$	W
Pulse frequency	1/7.2	Hz

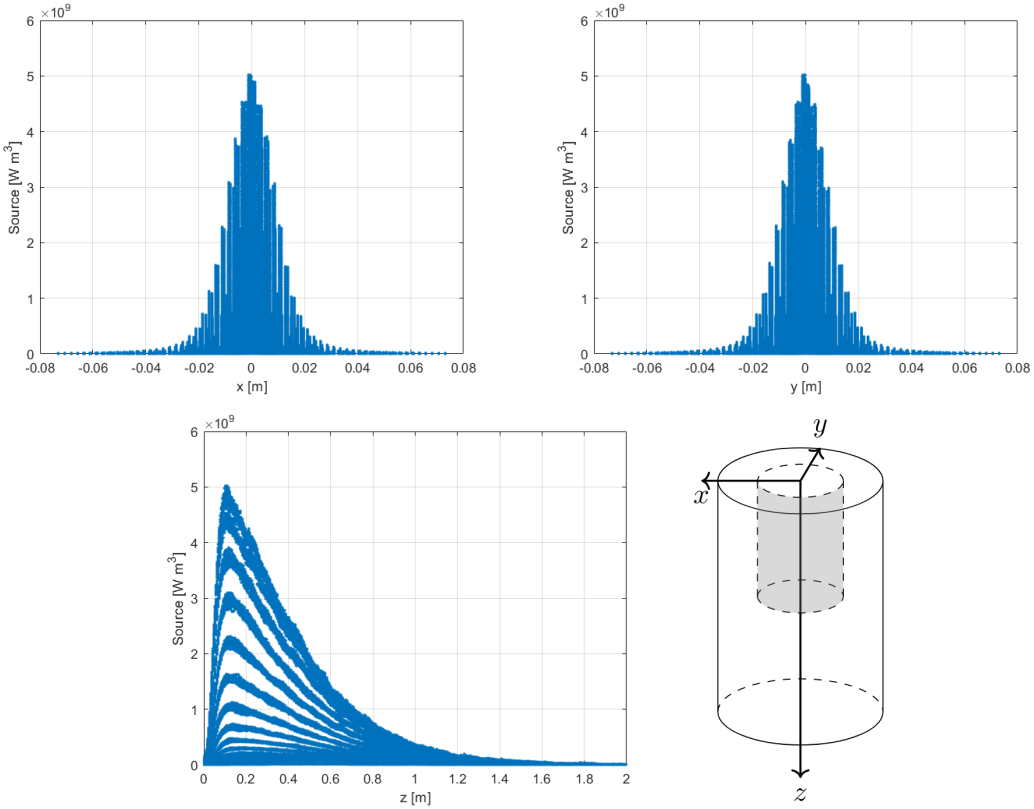

Figure 3: Source distribution along the (x,y,z) axis (top left, top right and bottom left, respectively); coaxial narrow cylinder where the source is concentrated (bottom right).

The spatial thermal source distribution is graphically shown in Figure 3 top and bottom left. Looking at the source volumetric deposition inside the cylinder domain, it is clear that the source distribution is non-zero only in a smaller coaxial cylinder near the section hit by the beam, around 1 meter long (from z-axis distribution) and with a 2 mm diameter (from (x,y)-axis distribution). This narrow area where the beam power reaches values of 10^9 is coloured in grey in the bottom-right section of Figure 3. Thus, a C++ algorithm has been implemented to reflect the source concentration in the computational mesh. To highlights the importance of the refinement in the source term discretization, Figure 4 presents the interpolation of the source term into two different mesh configurations, with cell sizes of 2 mm and 0.5 mm. Here, red dots symbolize the cell centroids while in blue the source points on a constant (x, y) plane. To obtain a better source discretization, improving its distribution near the centre of the duct, a transformation into polar coordinates has been done: the implemented algorithm performs a redefinition of the point inside the smaller duct to better interpolate the source values where they are most effective. The results of the point redistribution are depicted in Figure 5, moving from a non-optimized configuration (left) to an optimized one (right).

Figure 6 shows the volumetric source interpolations on a constant z-plane for the two different mesh discretizations. It illustrates how the mesh size influences the representation of thermal power within the liquid lead target volume. From their analysis, it is clear how a finer mesh

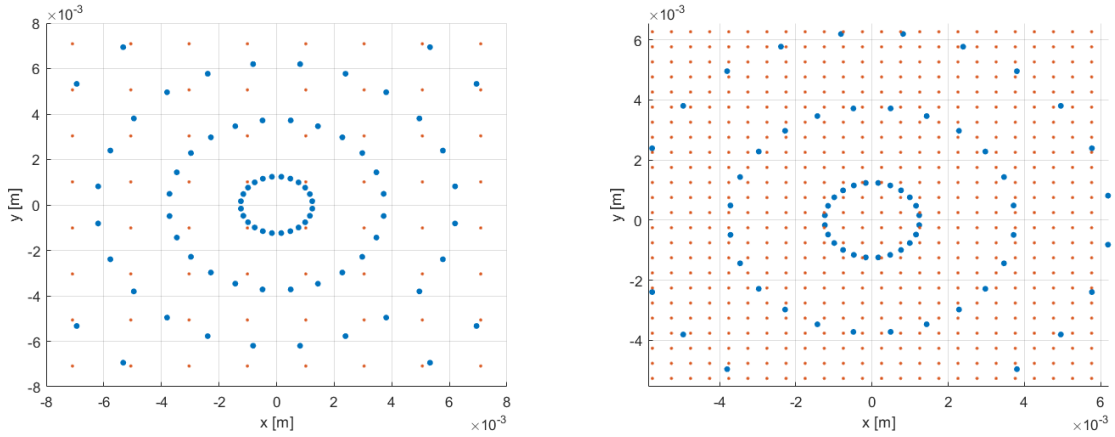

Figure 4: Thermal source implementation on a planar slice for two meshes with different discretization (2 mm, on the left; 0.5 mm, on the right). In red the cell centroids, while in blue the heat source points.

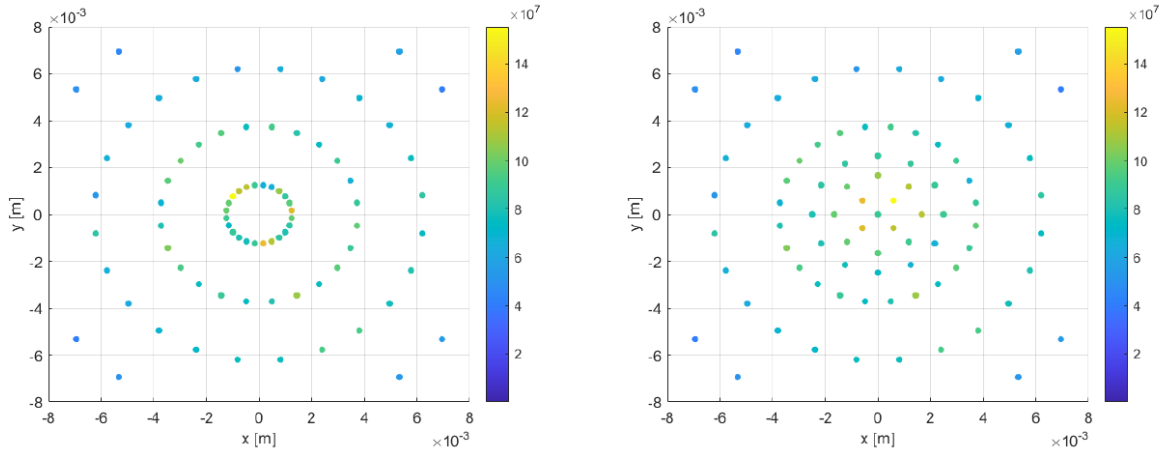

Figure 5: Proton beam source before and after the redistribution (left and right, respectively) on a constant z-plane.

allows a better distribution of the source on the whole axis length, while for a coarser mesh, the number of representative points is significantly lower. Then, to effectively implement the deposited beam power into the mesh, regardless of the chosen mesh refinement, the Body of Influence (BOI) mesh technique was employed. This feature allows the definition of sub-regions within the domain to which specific refinements or properties can be assigned. Therefore, these user-defined zones are here used to implement the thermal map: two different BOI have been created, coaxial to the 1-meter narrow cylinder defined in Figure 3, bottom right. The first is an external cylinder with 20 mm diameter and 2 mm mesh refinement, the second is an inner cylinder with 10 mm diameter and 1 mm mesh refinement. The results, in Figure 7, show good agreement between the implemented thermal heat map thanks to the BOI technique, the orange points, and the given FLUKA heat source data over the corresponding mesh points, in blue.

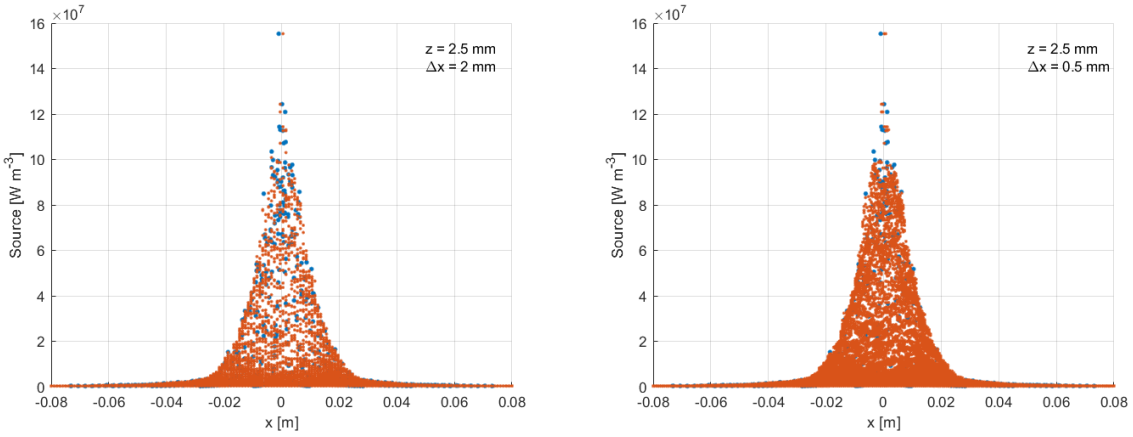

Figure 6: Volumetric thermal source interpolation on different sized mesh. On the left the 2 mm mesh while on the right the 0.5 mm mesh.

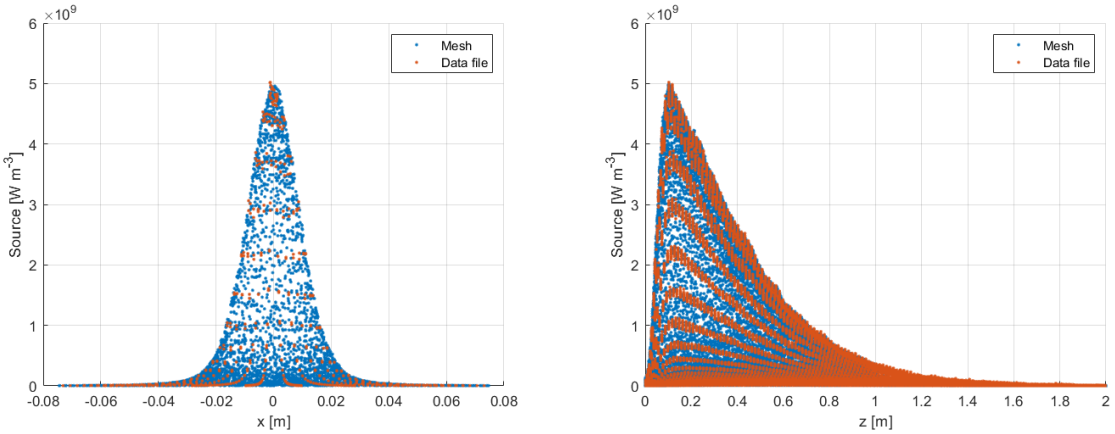

Figure 7: Comparison between the FLUKA data, in blue, and the interpolated source point with the BOI technique, in orange. x-plane (left) and z-plane (right).

5 CFD CODES

In this section, we briefly discuss the two Ansys codes, CFX and Fluent, which are selected for the CFD simulations being both industry standard for fluid flow, turbulent, and heat transfer simulations. We aim to conduct a comparative analysis and confirm the project's feasibility by applying both codes to the new baseline target simulation. Both codes discretize PDE equations using the finite volume method (FVM), evaluating the quantity of interest in control volume and using cell flux interpolations. Still, the difference is in the definition of the control volume. CFX exploits the Vertex-centered Method (VCM) where each computational cell is defined starting from the middle lines passing by the cell's border, with variables stored in the mesh nodes. Fluent, instead, uses the Cell-centered Method (CCM) in which the control volume are the cells itself, with variables stored in the cell's centroids. This difference between the codes is illustrated in Figure 8.

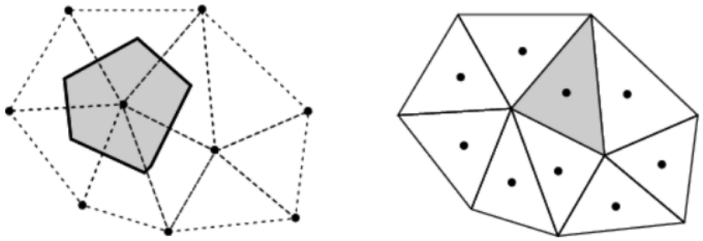

Figure 8: Vertex-centered method, on the right, and Cell-centered method, on the left.

The turbulence model and boundary conditions (BCs) have been chosen as similar as possible, to encourage a fair comparison between the two codes' results. Both codes simulate turbulence solving the well-known RANS (Reynolds-Averaged Navier-Stokes) equations. The turbulent model chosen for the closure of the equations is the $k - \omega\, SST$, considered one of the best among RANS models for the simulation of heavy liquid metals' behaviour [7]. An imposed mass flow rate of 42 kg/s is chosen as inlet BC, as well as 400 °C for the flowing liquid lead entering the cylinder duct. On the same patch, a homogeneous Neumann condition for the pressure is set. In contrast, a fixed pressure value is imposed on the outlet, where two homogeneous Neumann conditions are adopted for velocity and temperature. All the other patches are modelled as adiabatic walls: they are equipped with no-slip conditions for velocity and no heat flux conditions for the temperature. The meshing operation resulted in an unstructured mesh of 2.2 million nodes in CFX, for which the transient time stepping is set to $5 \cdot 10^{-4}$ s. For Fluent instead, a polyhedral unstructured mesh of 6.6 million nodes has been used, with a time step of $1 \cdot 10^{-3}$ s. Both meshes produce a $y^+ \leq 1$ at the walls, with Fluent also including an inflation layer of $1 \cdot 10^{-5}$ millimetre. Moreover, Fluent superimpose the inlet velocity condition thanks to the User Defined Function (UDF) feature.

6 NUMERICAL RESULTS

As previously stated, three different flow conditions are considered: (1) En_T, where only the energy equation with imposed motion is solved, and constant physical properties; (2) En_Tm, where only the energy equation with variable physical properties is solved; (3) En_full, where the complete simulation with variable properties, equation of motion, and energy are solved. Before proceeding with the code comparison, a single thermal Fluent simulation is conducted to investigate the effective differences between the temperatures among the three cases. The maximum and average volume temperature values are reported in Table 3.

Table 3: Maximum and average volume temperature profiles for the three cases.

Case	T max [K]	T ave [K]
En_T	1403	823
En_Tm	1463	829
En_full	1482	823

From this first analysis, we can see that the maximum temperature difference is between the constant property case and the full case. Nevertheless, being the average values very close to each other and the maximum values largely below the safety limits (around 520° under the lead boiling temperature) it is safe to consider for the following simulations the En_T case only. This results in obvious numerical advantages: avoiding the resolution of the complete simulation and considering lead physical properties as constant drastically reduces the computational time required for the running of simulations. With this assumption, the code comparison is conducted for both an isothermal case and a thermal transient scenario, using only the energy equation and constant physical properties(En_T). Concerning the isothermal case, the comparison between CFX and Fluent is reported in Figure 9, where the simulation results for velocity (v), pressure (p) and turbulent kinetic energy (k) are plotted on the middle axis of the channel. Here, Fluent is represented by the solid blue line while CFX with the solid red line.

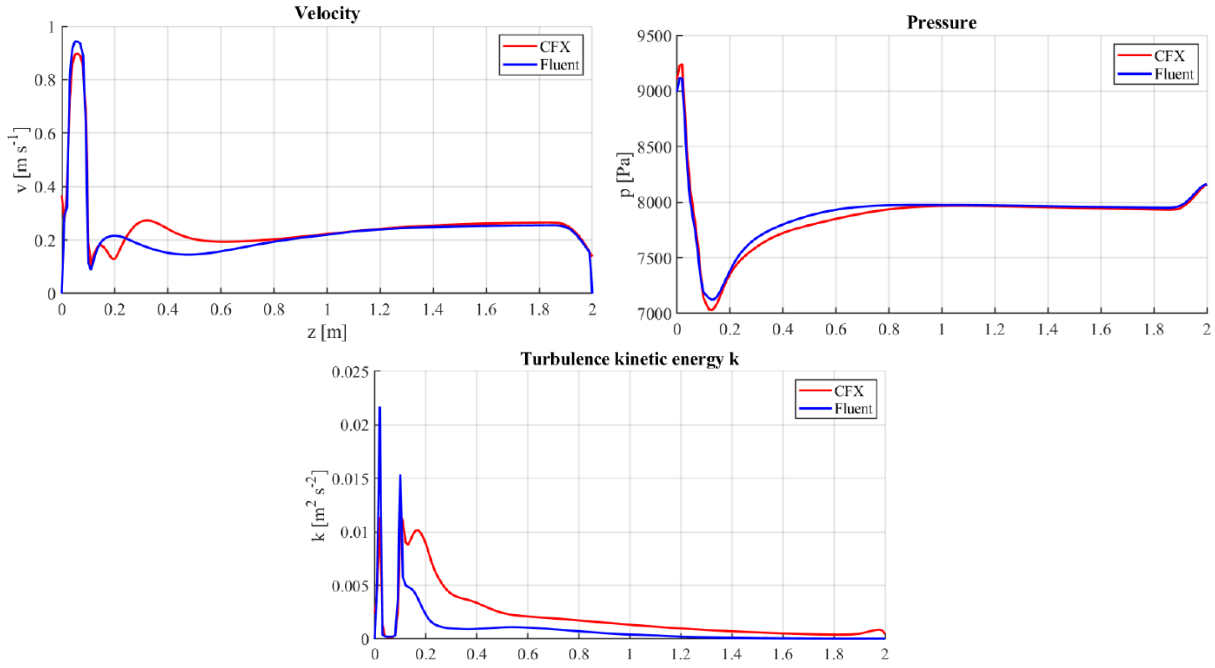

Figure 9: Plot of the isothermal simulation for the variable of interest. In solid red line, CFX code; in solid blue line Fluent code.

The plot trends show a good agreement between the codes, with the larger differences all concentrated in the pipe's initial region, in the transversal inlet duct area. This is probably due to the different boundary configurations and inlet velocity profiles, with Fluent providing it with a UDF function. Regarding the thermal transient simulation, the differences in temperature behaviour in CFX and Fluent are highlighted in Figure 10 for two consequent beam pulses. First, the maximum temperature inside the cylinder volume reached after the two beams is the same for both Fluent and CFX. Therefore, the thermo-hydraulic of the second peak is not influenced by the residual effect of the first pulse. This is also evidenced by the peak temperature at the outlet, which is reached before the second pulse. Moreover, the greatest temperature differences are at the channel wall ($\sim 55°$) and inside the domain volume ($\sim 32°$). Considering the nominal

magnitude of the temperature fields, these differences between the two codes can be regarded as acceptable being one order of magnitude lower: with these considerations is possible to affirm that the two codes produce comparable results regarding the target design and performance.

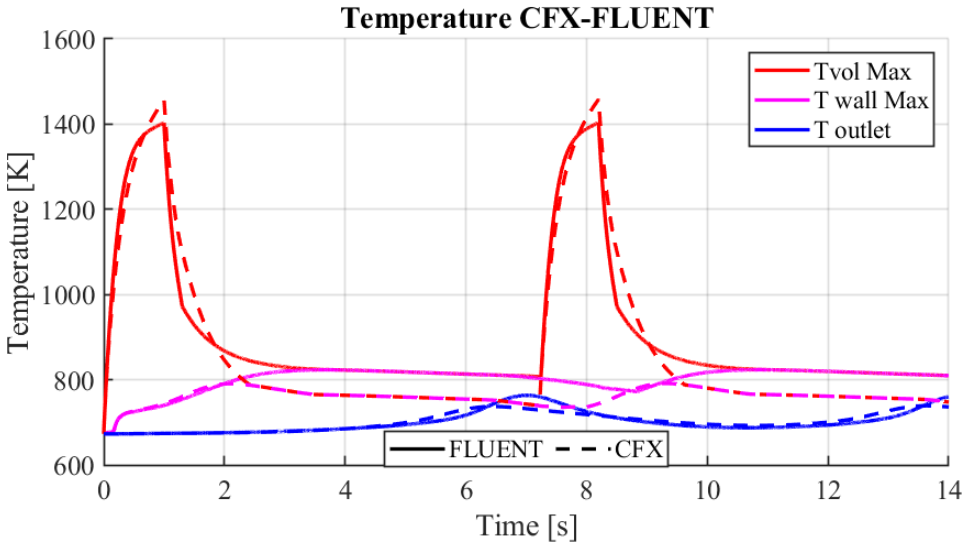

Figure 10: Average and maximum temperature profiles inside the volume, red lines; at the duct walls, pink lines; at the pipe outlet, blue lines. Comparison between Fluent results (solid lines) and CFX (dashed lines).

7 CONCLUSIONS

In this work, a new baseline target for the SPS-BDF has been proposed, to replace the current solid-state target with a flowing liquid lead one, ensuring a better disposal of the heat flux given by the proton beam pulse. CFD simulations have been conducted with two industry-standard codes, considering a mass flow rate of 42 kg/s and turbulent Prandtl number thanks to empirical correlations to overcome the problem of CFD models for low Prandtl numbers.

The thermo-hydraulic analysis theoretically confirms the idea's feasibility, resulting in peak values $\sim 530°$ below the lead boiling point, avoiding any possibility of local vaporization or flashing phenomena. Moreover, Fluent and CFX show comparable results, with a wall maximum temperature of 823 K and 793 K respectively. The two also highlight the temperature independence on the proton beam deposition frequency with this specifications.

Future development on this topic will be considered, investigating how a change in the inlet geometry would affect the temperature field, together with a comprehensive stress analysis on the target and experimental campaigns to understand the liquid lead-beam interaction better.

REFERENCES

[1] Alekhin, S. et al. "A facility to Search for Hidden Particles at the CERN SPS: the SHiP physics case." Reports on progress in physics 79.12 (2016): 124201

[2] Franqueira Ximenes, Rui, et al. "JACoW: CERN BDF Prototype Target Operation, Removal and Autopsy Steps." JACoW IPAC 2021 (2021): 3559-3562.

[3] Lopez Sola, E., et al. "Beam impact tests of a prototype target for the beam dump facility at CERN: Experimental setup and preliminary analysis of the online results." Physical Review Accelerators and Beams 22.12 (2019): 123001.

[4] Nuclear Energy Agency, "Handbook on Lead-bismuth Eutectic Alloy and Lead Properties, Materials Compatibility, Thermalhydraulics and Technologies", OECD (2015); p. 950.

[5] Cheng, X; Tak, N.i; "Investigation on turbulent heat transfer to lead-bismuth eutectic flows in circular tubes for nuclear applications"; Nuclear Engineering and Design (2006) ,236, 385-393

[6] Ahdida, Claudia, et al. "New capabilities of the FLUKA multi-purpose code." Frontiers in Physics 9 (2022): 788253.

[7] Barbi, Giacomo, Valentina Giovacchini, and Sandro Manservisi. "A New Anisotropic Four-Parameter Turbulence Model for Low Prandtl Number Fluids." Fluids 7.1 (2021): 6.